

A Novel Femtosecond Laser-Assisted Method for the Synthesis of Reduced Graphene Oxide Gels and Thin Films with Tunable Properties

Khaled H. Ibrahim, Mehrdad Irannejad,* Mojtaba Hajialamdar, Ali Ramadhan, Kevin P. Musselman, Joseph Sanderson, and Mustafa Yavuz

Graphene and its functionalized derivatives are unique and multifaceted novel materials with a wide range of applications in chemistry, healthcare, and optoelectronic engineering. 3D graphene materials exhibit several advantages over 2D (monolayer) graphene for a variety of devices applications. Here a novel and effective room temperature technique is introduced to convert an aqueous graphene oxide solution into a reduced graphene oxide gel with tunable physical and chemical properties comparable to a monolayer graphene sheet, without the need for any additives or chemical agents. The femtogel is synthesized by exposing an ultrahigh concentration graphene oxide solution with single-layer flakes to high intensity femtosecond laser pulses. The femtosecond laser beam is focused on the air/aqueous solution interface to enhance the vaporization of functional groups and water, enabling femtogel formation. By controlling the pulsed laser intensity, beam focal parameters, and pulse duration, it is possible to produce several milliliters of femtogel in as little as 8 min. Through initial optimization of the irradiation parameters, a thin film is produced from a femtogel that demonstrates a surface roughness less than 6 nm, and more than 95% reduction in OH absorbance, as compared to a thin film produced from the unexposed graphene oxide solution.

1. Introduction

Graphene oxide hydrogel and gel are two derivatives of graphene oxide that have attracted general interest due to their immense potential for application in a wide range of engineering fields

such as bioengineering, micro- and nanoelectronics, chemical engineering, and materials engineering.^[1] These gels have been extensively used as a soft material in many applications including drug delivery, tissue engineering, sensor engineering, and actuator device development.^[2] Graphene-oxide-gel-based materials provide several advantages over conventional graphene oxide sheets such as a large surface area, as well as high electrical and thermal conductivities.^[3]

To meet the large demand for graphene oxide gels, the main challenge is to effectively convert a solution of aqueous graphene oxide into a soft graphene oxide hydrogel, sol-gel, or gel with tunable properties. The self-assembly method is the main fabrication technique used for producing 3D graphene oxide gels from a 2D aqueous graphene oxide solution.^[4–13] In this conventional method, the gelation of the graphene oxide sheets is achieved by introducing appropriate molecular interactions, including electrostatic inter-

actions, π – π stacking, and hydrogen bonding.^[14–16] Notably, the introduction of a chemical agent such as polymer is an essential requirement of this technique to produce a graphene oxide gel from an aqueous graphene oxide solution.^[17] The chemical agent acts as a physical cross-linker between the graphene oxide sheets. The physical and electrical properties can be altered by using different types of cross-linkers such as nickel foam,^[18] pluronic copolymer,^[15] ferrocene,^[6] DNA,^[13] poly(vinyl alcohol) (PVA), as well as divalent and trivalent metals such as Ca^{2+} , Mg^{2+} , Cu^{2+} , and Ce^{3+} .^[17] The cross-linking agents are dispersed in the graphene oxide solution and result is an increase in the amount of suspended graphene oxide sheets in the solution.^[14] Nonionic surfactants (e.g., P-123 and Brij 700^[17]) are also used as modifiers in the conversion of a graphene oxide solution into a graphene oxide hydrogel or gel.

Recently, Compton and co-workers^[19] reported 3D graphene oxide hydrogel formation using ultrasonification without any additives. It was reported that ultrasonification of precursor graphene oxide sheets reduces the 2D graphene oxide sheet dimensions by breaking them into smaller units that lack carboxyl functional groups as a stabilizer in water. The broken graphene

K. H. Ibrahim, Dr. M. Irannejad, Dr. K. P. Musselman,
Prof. M. Yavuz

Waterloo Institute for Nanotechnology
University of Waterloo

Waterloo N2L 3G1, ON, Canada
E-mail: Mehrdad.Irannejad@uwaterloo.ca

Dr. M. Irannejad, Dr. K. P. Musselman, Prof. M. Yavuz
Department of Mechanical and Mechatronics Engineering
University of Waterloo

Waterloo N2L 3G1, ON, Canada

Dr. M. Hajialamdar, Dr. A. Ramadhan, Dr. J. Sanderson
Department of Physics and Astronomy
University of Waterloo
Waterloo N2L 3G1, ON, Canada

DOI: 10.1002/admi.201500864



oxide sheets stack with each other through π -stacking and electrostatic forces. Using this method, a graphene oxide hydrogel was formed in 30 min. Unfortunately, the hydrogel had more than 96% water and only 4% carbon content, resulting in poor electrical properties unsuitable for electronic-based devices such as N/MEMS, sensors, and actuators. Compton and co-workers improved the mechanical and electrical properties of the fabricated hydrogel by extending the sonification process up to 120 min, but the carbon contents was still less than 10%.

Furthermore, graphene oxide hydrogels and graphene oxide gels fabricated using self-assembly and ultrasonification methods contain porous structures^[14] that increase the resistivity of thin films formed using these materials and hence limit their applications.

The intrinsic properties of a graphene oxide gel can be improved by engineering the hydroxyl and carboxyl functional groups during the fabrication process. This possibility has led to increasing interest in graphene oxide gels without porous structures. Thus, it is crucial to reduce the graphene oxide solution during its conversion to a gel to enhance the electrical and thermal conductivity of the resulting material.

In this paper, we report for the first time, a novel and effective method for the conversion of an aqueous graphene oxide solution into a reduced graphene oxide gel that is capable of producing thin and dense films. The gels are formed using femtosecond laser irradiation ("femtogels") without any additives or chemical agents and can display more than 95% reduction in OH concentration (as compared to the graphene oxide solution). In this novel technique, the femtosecond laser beam is focused on the air/aqueous solution interface and the

femtogel (reduced graphene oxide gel), is formed in as little as 8 min at room temperature. Furthermore, by varying the irradiation conditions (laser pulse energy, focal length, irradiation time, etc.) we demonstrate that it is possible to tune the chemical and physical properties of the fabricated femtogel.

2. Results and Discussion

2.1. Femtogel Formation

An ultrahigh concentration aqueous graphene oxide solution with single-layer flakes ranging in size from 0.5 to 5 μm was irradiated by pulses from a high intensity femtosecond laser (pulse energy of 250 μJ , pulse duration of 100 fs and focal length of 5 cm). When the laser beam was focused inside the graphene oxide solution, as illustrated in Figure 1a, a visible white filament a few millimeters in length was observed, as shown in the inset of Figure 1a. The nature of the filament formation was reported previously.^[20–22] The filamentation affects the irradiation process by first, clamping the peak intensity on the order of $4 \times 10^{13} \text{ W cm}^{-2}$, depending on the nonlinear refractive index of the medium. Second, an extension of the interaction volume occurs, by up to three orders of magnitude compared to that expected from the Rayleigh range and focal spot size of a standard geometric focus. Focusing the laser beam at the air/graphene oxide solution interface instead, (Figure 1b) avoided the filamentation and supercontinuum generation in the graphene oxide solution, replacing it with a bright spot. Self-focusing in air is still possible in this setup, but this

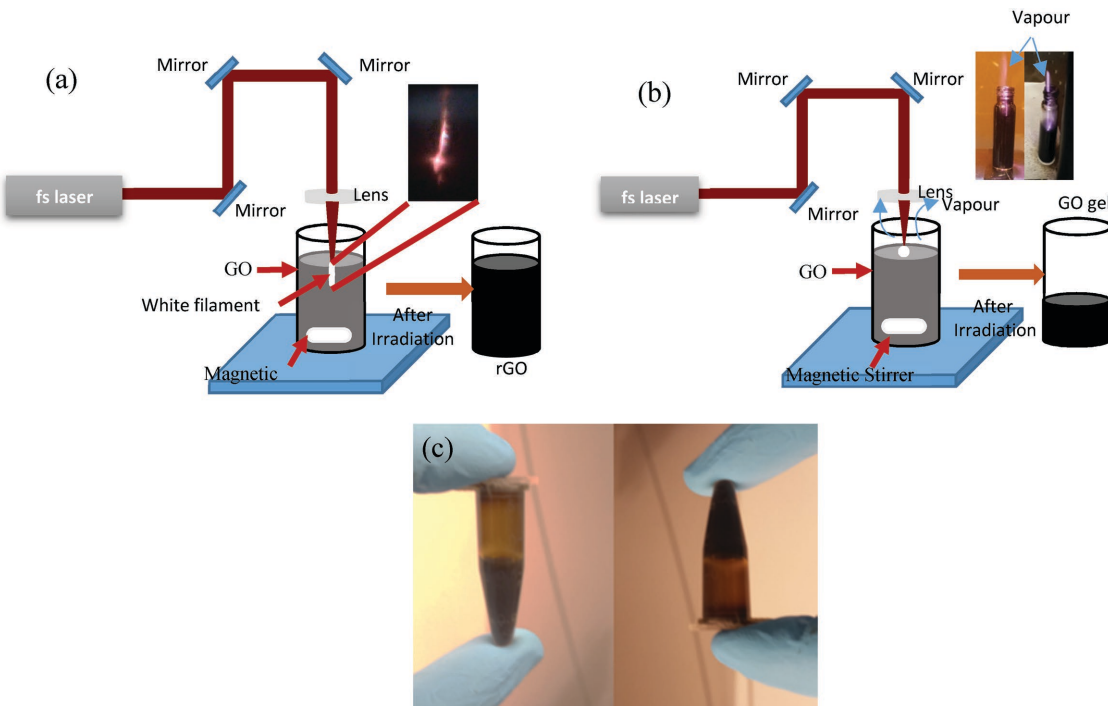


Figure 1. Schematic diagram of vial containing graphene oxide solution showing a) laser focused within the solution, supercontinuum generation effect (white filament) due to self-focusing, and reduced graphene oxide (rGO) formation, b) laser focused at surface and reduced graphene oxide gel (femtogel) formation. The inset shows the vaporization effect from the surface and femtogel formation. c) Acquired femtogel after laser irradiation.

only increases the intensity at the air/liquid interface. Taking into account only geometric considerations, it is estimated that a spot size of 10 μm can be generated^[20–22] at the air/graphene oxide solution interface for a laser pulse with energy of 250 μJ and duration of 100 fs, which results in a peak intensity on the order of $4 \times 10^{15} \text{ W cm}^{-2}$ and an electric field magnitude on the order of 10^9 V m^{-1} .

Focusing the laser beam inside the graphene oxide solution (as in Figure 1a) to produce an effective pulse intensity of $4 \times 10^{13} \text{ W cm}^{-2}$ yielded a reduced graphene oxide solution with a volume comparable to that of the initial solution, in a similar manner as reported previously.^[23–27] The stability of the water content throughout the laser exposure can be assigned to covalent bond formation between the H^+ ions in the exposed solution and free OH radicals from the reduced graphene oxide sheets, which result in the formation of H_2O and H_2O_2 molecules. By focusing the laser beam at the graphene oxide solution/air interface (as in Figure 1b), which increased the pulse intensity to $4 \times 10^{15} \text{ W cm}^{-2}$, more than 50% of the water content of the 5 mL of graphene oxide solution was vaporized due to nonthermal surface ablation and explosive ablation at the surface over a 7 h period. This resulted in the formation of a high viscosity femtogel instead of a reduced graphene oxide aqueous solution as shown in Figure 1c.

The formation of the femtogel can be understood by considering the chemical properties of graphene oxide sheets and their dispersion mechanism in solution. It is known that graphene oxide sheets are hydrophilic at the edges.^[9] Hence, they are dispersed in the water through covalent bonds between the carboxyl functional groups at the edges and the in-plane carbonyl and hydroxyl functional groups in the graphene oxide sheets,^[22,28] as illustrated in Figure 2a. The short-duration femtosecond laser pulses are expected to result in coulomb explosion in the aqueous graphene oxide solution

and fracturing of the graphene oxide sheets, as shown in Figure 2b. As for Campton's sonication method, the resulting sheet fragments are expected to have very small dimensions, which do not contain the carboxyl functional groups.^[19] It is therefore expected that when the laser is focused at the surface of the solution, the carboxyl functional groups, the in-plane hydroxyl groups and the water in the aqueous graphene oxide solution are removed in the form of vapor. This results in the observed reduction in solution volume and the presence of more sp^3 rather than sp^2 hybridized molecules, with 25% and 33% S-orbital character respectively.^[28,29] The reduction in hydrogen covalent bonds, combined with weak repulsion electrostatic forces between the reduced graphene oxide sheets, is expected to result in stacking of the sheets through van der Waals forces and $\pi-\pi$ stacking forces^[14] (Figure 2c), producing the observed graphene femtogel.^[30] Thus, an aqueous graphene oxide solution can be converted into a femtogel by removing the carboxyl and hydroxyl functional groups, the in-plane hydroxyl groups and water content from the surface of the solution.

By using femtosecond laser pulses with a pulse energy of 2 mJ, pulse duration of 35 fs and focal length of 5 cm, the pulse intensity and induced electric field were increased to approximately $8 \times 10^{16} \text{ W cm}^{-2}$ and $8 \times 10^{11} \text{ V m}^{-1}$, respectively. This resulted in a reduction in the irradiation time required to convert 5 mL of the aqueous graphene oxide solution into a femtogel from 7 h to 58 min. In addition to increasing the pulse intensity, increasing the focal length from 5 to 10 cm and reducing the treated solution volume from 5 to 1.5 mL further reduced the irradiation time required to produce the femtogel to only 8 min. These gel formation times are summarized in Table 1.

Importantly, it was found that the physical and chemical properties of the acquired femtogel, as well as its surface

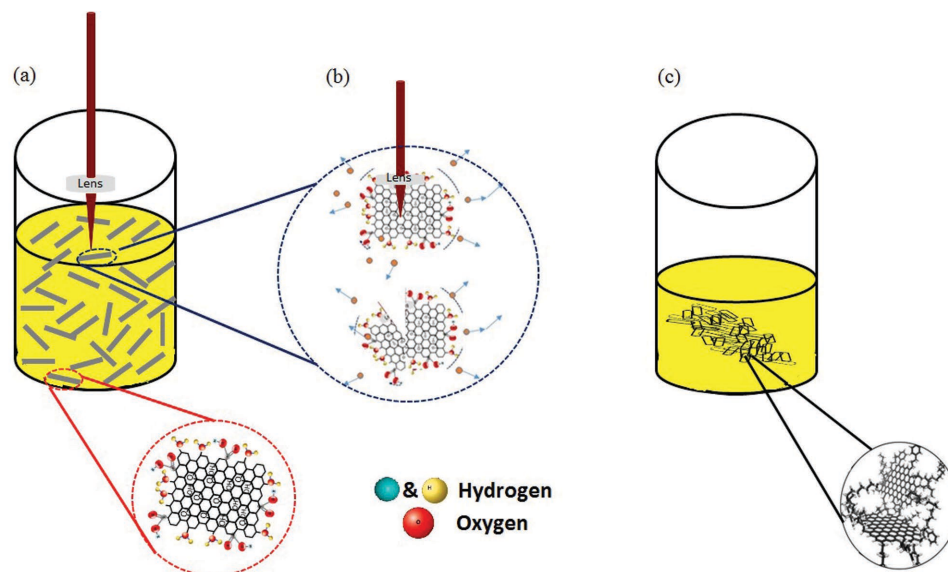


Figure 2. Schematic diagram of the femtogel formation. a) Graphene oxide sheets in solution with carboxyl functional groups at the edges and in-plane carbonyl and hydroxyl functional groups. b) The femtosecond laser beam strikes the graphene oxide sheets producing smaller fragments with pristine edges free from carboxyl and hydroxyl groups. c) Functional groups and water are ejected from the surface of the solution as vapor, and stacking and aggregation of the reduced graphene oxide sheet fragments occurs, resulting in femtogel formation.

Table 1. Laser parameters, irradiation times, and solution volumes used for reduced graphene oxide (rGO) and femtogel formation.

Sample	Pulse energy [mJ]	Pulse duration [fs]	Focal length [cm]	Exposure time	Volume [mL]
rGO	0.250	100	5	7 h	5
	0.250	100	5	7 h	5
Graphene femtogel	2	35	5	58 min	5
	2	35	5	20 min	1.5
	2	35	10	8 min	1.5

morphology when deposited as a thin film, can be controlled by varying the laser pulse energy, pulse duration, beam focal length, and by varying the irradiation time, allowing the resulting gel to be engineering for different applications.

2.2. Fourier Transform Infrared Spectroscopy

Freestanding thin films were produced from the femtogels and graphene oxide solutions as detailed in Section S1 of the Supporting Information. The FTIR absorbance spectra in Figure 3 demonstrate the ability to control the concentration of hydroxyl and carboxyl groups in films produced from the femtogel by varying the pulse intensity, focal length, and more extensively by varying the irradiation time.

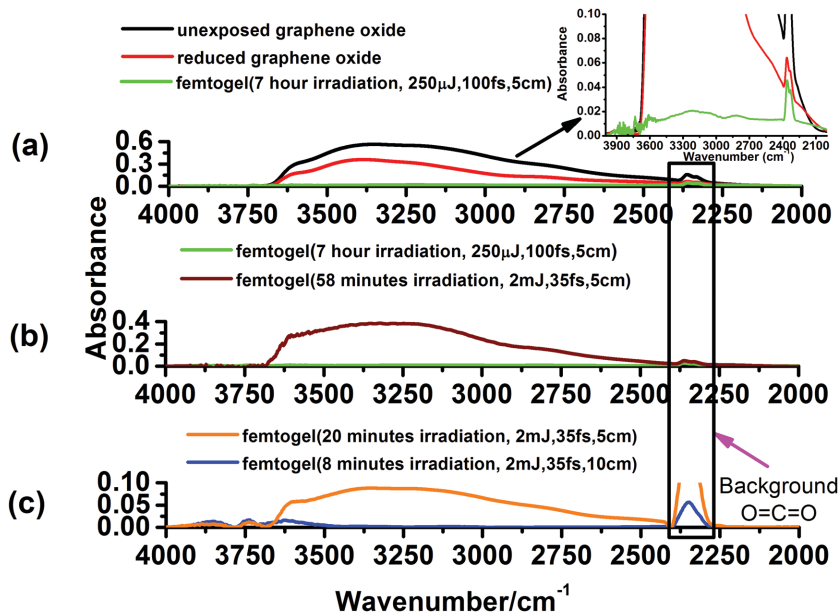


Figure 3. Freestanding thin film FTIR absorbance spectra. a) Comparison of a (—) graphene oxide thin film, (—) reduced graphene oxide film, and (—) femtogel film (the reduced graphene oxide solution and femtogel were irradiated 7 h using a pulse energy of 250 μJ, pulse duration of 100 fs, focal length of 5 cm, and solution volume of 5 mL). b) Comparison of films made from femtogels formed in (—) 7 h using a 0.250 mJ pulse energy, pulse duration of 100 fs and (—) 58 min using a pulse energy of 2 mJ and pulse energy of 35 fs (focal length of 5 cm and solution volume of 5 mL for both). c) Comparison of films made from femtogels formed in (—) 20 min using a focal length of 5 cm and (—) 8 min using a focal length of 10 cm (pulse energy of 2 mJ, pulse duration of 35 fs, and solution volume of 1.5 mL for both). All FTIR spectra were recorded using a 1" freestanding thin film. All details and conditions are summarized in Table 1.

Figure 3a shows the spectra of thin films made using a reduced graphene oxide solution and femtogel (both synthesized with a pulse energy of 250 μJ, pulse duration of 100 fs, focal length of 5 cm, and irradiation time of 7 h), as well as a film made using the unexposed graphene oxide solution. It can be observed that the intensity of the broad OH⁻ absorbance is 36% smaller for the film produced using the reduced graphene oxide solution (red curve) than the film produced using the unexposed graphene oxide solution (black curve). The OH⁻ absorption peak width of the reduced graphene oxide was also reduced by 221 cm⁻¹ as a result of the 7 h laser treatment. This could be due to changes in the chemical nature of the hydroxyl groups and a reduction in the amount of OH⁻ in the fabricated reduced graphene oxide film. As can be seen from this figure, the OH⁻ absorbance intensity of the femtogel film (green curve) was significantly reduced compared to the other films (i.e., more than 95% lower than the film made from unexposed graphene oxide solution). The removal of hydroxyl groups is consistent with the gel formation mechanism proposed in Section 2.1. However, it is important to note that while some of these oxygen and OH⁻ radicals are ejected from the solution in water vapor form (Supporting Movie 2, Supporting Information), the Raman and X-ray photoelectron spectroscopy (XPS) results presented in the following section indicate that other liberated oxygen results in the formation of C=O bonds. The vibration frequency of the asymmetrical stretching O=C=O mode was recorded in the range of 2330 to 2362 cm⁻¹ and is assigned to background CO₂ contamination.^[31]

Figure 3b shows the hydroxyl absorbance for films produced from femtogels formed in 58 min and 7 h using 5 mL of solution. As discussed in detail in Section S2 of the Supporting Information, the absorbance for the 7 h femtogel was 35× smaller than that of the femtogel formed in 58 min, demonstrating that the OH content can be tuned via the gel formation time/laser pulse energy. As noted previously, the femtogel can be formed in less than 58 min by reducing the initial graphene oxide solution volume from 5 to 1.5 mL and increasing the laser focal length (summarized in Table 1). The FTIR spectra of the femtogel formed in 20 min with a focal length of 5 cm and the femtogel formed in 8 min with a focal length of 10 cm (both with pulse energies of 2 mJ, pulse durations of 35 fs, and graphene oxide solution volumes of 1.5 mL) are shown in Figure 3c. The amount of OH⁻ absorbance in the graphene femtogel formed in 8 min was 36 times lower than that formed in 20 min, demonstrating that in addition to the gel formation time, the focal length of the laser irradiation can also be used to control the OH⁻ content. These

functional groups and dispersed water molecules alter the hexagonal structure of the carbon basal plane and, therefore, the intrinsic physical and electrical properties of the graphene oxide and reduced graphene oxide sheets.^[32,33] The structural alteration of the carbon basal plane could be confirmed by UV/vis spectroscopy in the future. The high concentration graphene oxide solution and femtogels produced in this work had high optical densities that prevented absorption measurement. The demonstrated ability to control the OH⁻ content of the femtogels therefore allows their optimization for different applications.

2.3. Raman Spectroscopy

The main recorded features in the Raman spectra of the thin films deposited on silicon substrates from unexposed graphene oxide solution, reduced graphene oxide solution, and the femtogels were the D band (at $\approx 1350\text{ cm}^{-1}$) and G band (at $\approx 1595\text{ cm}^{-1}$) as shown in Figure 4a,b and summarized in Table 2. The appearance of the D band is attributed to scattering effects between the defects sites and phonons that result in the sp² breathing mode within the basal plane of the graphene oxide sheets, while the appearance of the G band was attributed to the planar configuration of sp²-bonded carbon.^[34] Two weaker peaks were also recorded at wavenumbers of 2699 and 2930 cm⁻¹ that were attributed to the 2D and D+G bands,^[14] respectively.

The quality of the femtogel films was generally assessed by calculating the I_D/I_G ratio also known as the defect ratio.^[33,35]

The defect ratio of the unexposed graphene oxide film, reduced graphene oxide film and films made from the femtogels were calculated and summarized in Table 2 and are shown in Figure 4c. Figure 4a compares the Raman spectra of unexposed graphene oxide, reduced graphene oxide, and femtogel (7 h formation time) films. Increasing the number of dislocations and defect sites in the aromatic planes through laser irradiation has previously been shown to result in an increase in the defect ratio.^[36,37] It was found here that the defect ratio increased from 0.86 in the unexposed graphene oxide thin film to 0.96 in the thin film made from the femtogel formed in 7 h, as shown in the lower portion of Figure 4c. An increase in the number of defect sites and dislocation sites with laser irradiation was confirmed by XPS analysis (Section S3 of Supporting Information) where it was found that the intensity of the signal corresponding to C—O bonds was significantly larger (relative to the C—C bond signal) in the thin films made from the femtogels than in a thin film deposited from the unexposed graphene oxide solution.^[29]

With increasing defect ratio, it is expected that the sp² domains become smaller and more distorted, until they break up and produce more sp³ domains.^[38] Replacing the dislocated carbon atom in the basal plane with an oxygen atom provides a linkage with neighboring graphene sheets through the C—O—C bonds, likely resulting in cluster formation and aggregation of graphene flakes. Thus while the defect ratio can be

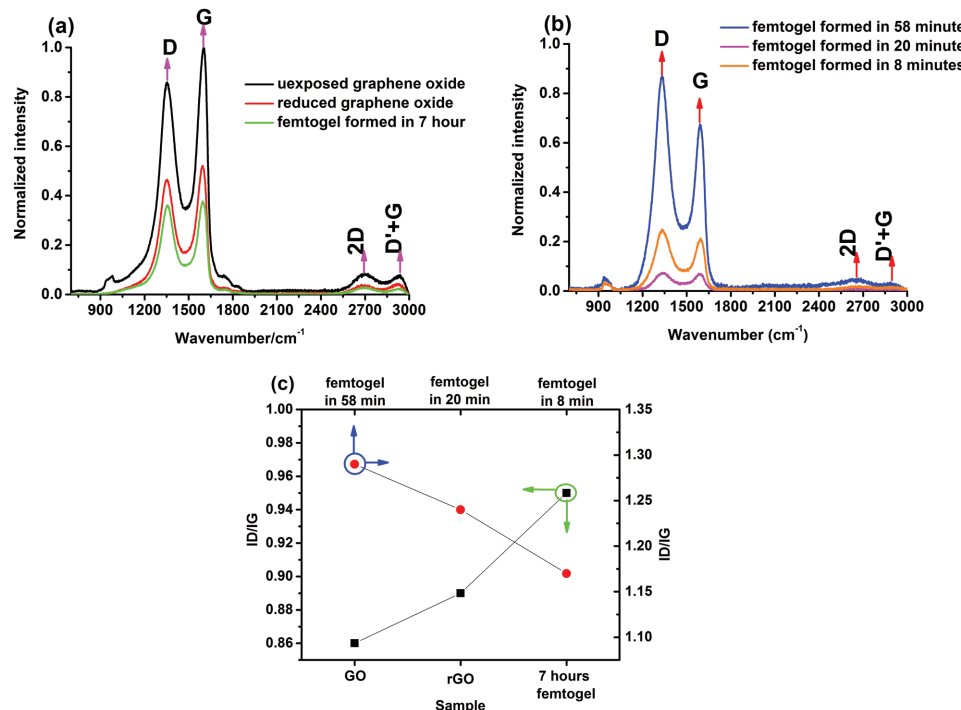


Figure 4. The recorded Raman spectra of thin films formed from a) unexposed graphene oxide, reduced graphene oxide, and femtogel synthesized in 7 h (pulse energy of 250 μJ , pulse duration of 100 fs, focal length of 5 cm, and solution volume of 5 mL); and b) femtogels formed using a pulse energy of 2 mJ and pulse duration of 35 fs in 58 min (focal length of 5 cm and solution volume of 5 mL), 20 min (focal length of 5 cm and solution volume of 1.5 mL), and 8 min (focal length of 10 cm and solution volume of 1.5 mL). c) The calculated defect ratios of the films shown in a) and b). The Raman spectra were recorded using an excitation wavelength of 632.8 nm and a power of 4.5 mW cm^{-2} . All Raman spectra were normalized based on the recorded intensity of the unexposed graphene oxide. All spectra were recorded from 1 cm \times 1 cm samples.

Table 2. The recorded D, G, and 2D band positions, relative intensities, defect ratios (I_D/I_G) and I_{2D}/I_G ratios of thin films formed from the unexposed graphene oxide (GO) solution, reduced graphene oxide (rGO) solution irradiated for 7 h, and femtogels formed in the range of 8 min to 7 h.

Sample	D		G		2D		I_D/I_G	I_{2D}/I_G
	Position [cm ⁻¹]	Intensity	Position [cm ⁻¹]	Intensity	Position [cm ⁻¹]	Intensity		
GO	1352	0.86	1601	1	2699	0.08	0.86	0.09
rGO	1351	0.46	1593	0.52	2700	0.04	0.89	0.09
7 h femtigel	1354	0.36	1595	0.38	2699	0.03	0.96	0.07
58 min femtigel	1333	0.87	1590	0.67	2647	0.05	1.29	0.07
20 min femtigel	1333	0.087	1586	0.070	2651	0.02	1.24	0.09
8 min femtigel	1337	0.25	1603	0.21	2675	0.08	1.17	0.08

used to assess the quality of the material, increasing the defect ratio appears to be advantageous in that it facilitates the formation of femtigel.

The Raman spectra of the femtogels formed in the range of 8 to 58 min using a 2 mJ pulse energy are compared in Figure 4b and the calculated defect ratios are reported in the upper portion of Figure 4c and in Table 2. Since the femtogels are formed by stacking the reduced graphene oxide sheets, the G band is shifted toward larger wavenumber (more graphitic structure). These data emphasize that the defect ratio depends on multiple irradiation parameters, including irradiation time, focal length, and pulse energy. The Raman spectroscopy shows that defects were most prevalent in the femtigel formed in 58 min (defect ratio of 1.29). When the gel formation time was decreased from 58 min to 20 min by decreasing the solution volume from 5 to 1.5 mL, the defect ratio decreased from 1.29 to 1.24. Furthermore, when the focal length was increased from 5 to 10 cm to further reduce the femtigel formation time to 8 min, a reduction in the defect ratio (to 1.17) resulted. This may be attributed to the larger processing volume due to the larger focal length producing lower defects such as vacancies, Stone-Wales defects, and impurities. The femtigel with the lowest observed structural disorder and defect ratio was that formed in 7 h with a 0.250 mJ pulse energy (shown in Figure 4a), with a defect ratio of 0.96 as detailed in Table 2 and shown in Figure 4c. Thus, it is clear that significant opportunity exists to control the defect ratio of the femtogels reported here, by controlling the various irradiation parameters.

2.4. X-ray Diffraction Analysis

XRD analysis was utilized to study the structural properties of the stacking layers in the thin films. Figure 5a shows the XRD data for the thin films produced from the unexposed graphene oxide solution, reduced graphene oxide solution, and femtigel formed in 7 h. By converting the graphene oxide solution into a femtigel, the interlayer spacing between each graphene oxide sheet was reduced from 0.75 to 0.72 nm, which is evident from a shift of 0.5° in the (001) diffraction peak to larger 2θ. This reduction in interlayer spacing is plotted in Figure 5c. Figure 5b shows the XRD data for thin films produced using femtogels with shorter formation times of 8 to 58 min (achieved using a 2 mJ pulse energy instead of

0.250 mJ). The existence of the second peak (i.e., (002) peak) in both Figures 5a,b indicates the presence of amorphous structure in the as-received graphene oxide solution, which is still in the reduced graphene oxide and femtigel thin films. Notably, in contrast to the smaller lattice spacing observed for the femtigel formed in 7 h, the position of the (001) peak was observed to shift downwards by approximately 2° (relative to the unexposed graphene oxide thin film) for the shorter gel formation times. This corresponds to an increase in the interlayer spacing from 0.75 to 0.86 nm for the (001) planes and a similar increase in spacing from 0.42 to 0.47 nm was observed for the (002) planes. Thus the femtogels formed in 8 to 58 min had an interlayer spacing larger than the unexposed graphene oxide thin film, reduced graphene oxide thin film, and even graphite.^[12,39–41] The increased interlayer spacing can be attributed to carbonyl groups (e.g., C—O bonds and C=O bonds with bond length of ≈0.14 and ≈0.12 nm, respectively, trapped between the graphene oxide sheets), and the corresponding expansion of the basal planes housing these bonds. This is consistent with the relative increase in C—O signals observed by XPS for the femtogels formed in 8 to 58 min (Section S3, Supporting Information).

The increase in the defect ratios (obtained from Raman spectra) and the number of dislocation sites of the thin films made from femtogels enhances the sp^3 hybridization within the reduced graphene oxide sheets of the femtogels. It is known that the carbon atoms in sp^2 hybridization have a trigonal planar structure with a bond angle of 120° while carbon atoms in the sp^3 hybridization formed a tetrahedral structure with a larger bond length than the trigonal planar structure^[42] as schematically shown in Figure 5d. The increase in the number of sp^3 hybridizations (e.g., C—O and C=O) in the produced femtogels results in an increased interlayer spacing in the femtigel thin films. All interlayer spacings are summarized in Table 3 and displayed in Figure 5c.

Fracture of the graphene oxide sheets and trapping of H₂O and H₂O₂ molecules, carbonyl bonds and carboxyl bonds between the sheets in the femtigel network also resulted in a reduction of the peak intensities recorded in the XRD patterns compared to that of the unexposed graphene oxide thin film, as seen in Figure 5a,b. It was found that the peak intensities of the films formed from the 7 h femtigel and 58 min femtigel were reduced by 50% and 95%, respectively, as compared to the unexposed graphene oxide thin film.

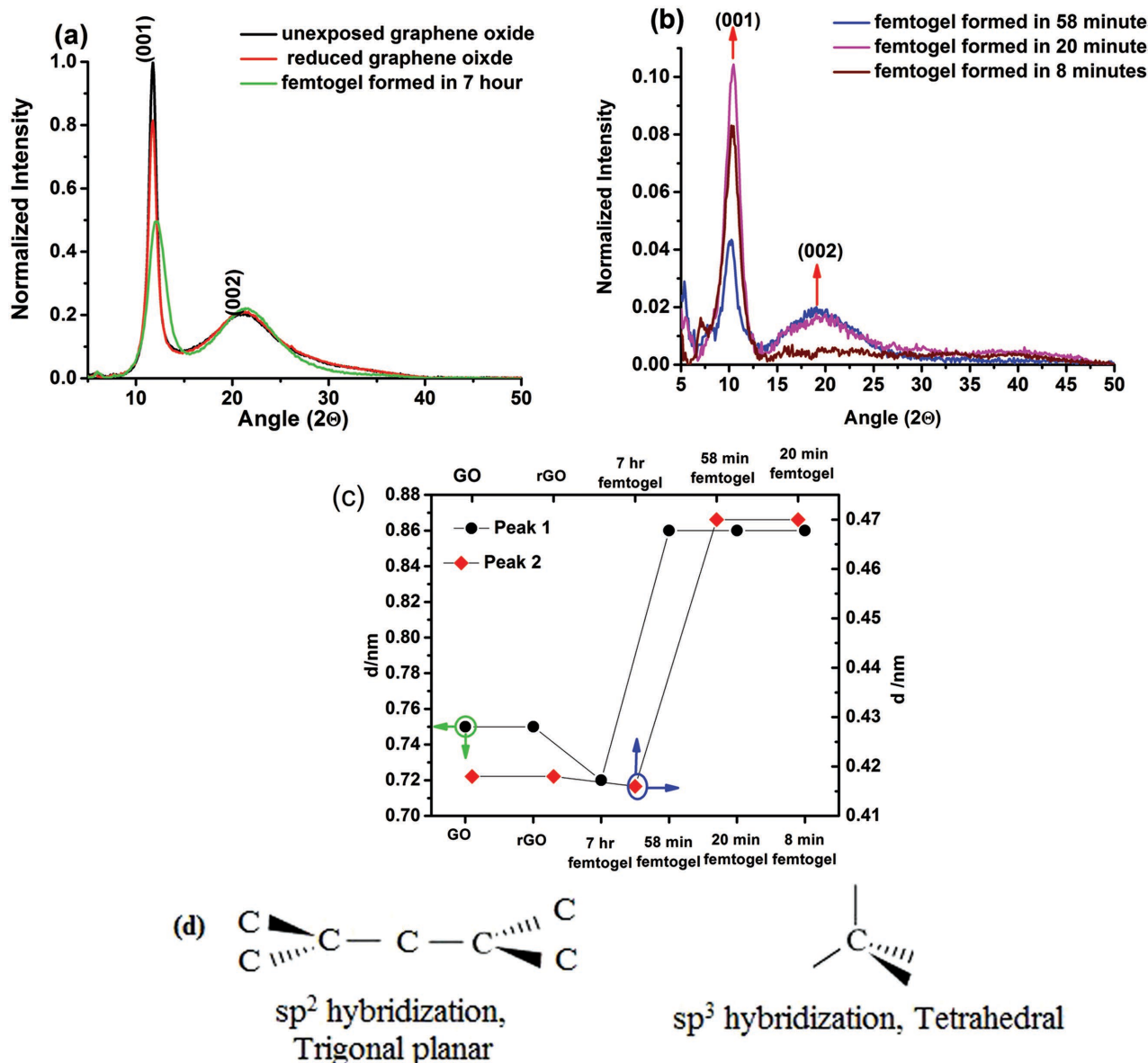


Figure 5. The recorded XRD patterns of thin films formed from a) unexposed graphene oxide, reduced graphene oxide, and femtogel synthesized in 7 h (pulse energy of $250 \mu\text{J}$, pulse duration of 100 fs , focal length of 5 cm and solution volume of 5 mL); and b) femtogels formed using a pulse energy of 2 mJ and pulse duration of 35 fs in 58 min (focal length of 5 cm and solution volume of 5 mL), 20 min (focal length of 5 cm and solution volume of 1.5 mL), and 8 min (focal length of 10 cm and solution volume of 1.5 mL). c) Calculated interlayer spacing of thin films shown in a) and b). d) Trigonal planar and tetrahedral structure of carbon atoms in sp^2 and sp^3 hybridization of a graphene oxide sheets.

Table 3. The recorded XRD (002) and (001) peak positions, intensities, and interlayer spaces in the thin films formed from graphene oxide (GO), reduced graphene oxide (rGO), and femtogels formed in the range of 8 min to 7 h .

Sample	(001) peak		(002) peak		Interlayer space [nm]	
	2θ	Intensity	2θ	Intensity	(001) peak	(002) peak
GO	11.75	1	21.25	0.21	0.75	0.42
rGO	11.75	0.81	21.35	0.21	0.75	0.42
7 h femtogel	12.25	0.49	21.35	0.22	0.72	0.41
58 min femtogel	10.25	0.04	19.05	0.02	0.86	0.47
20 min femtogel	10.45	0.10	19.05	0.02	0.86	0.47
8 min femtogel	10.25	0.08	-	-	0.86	-

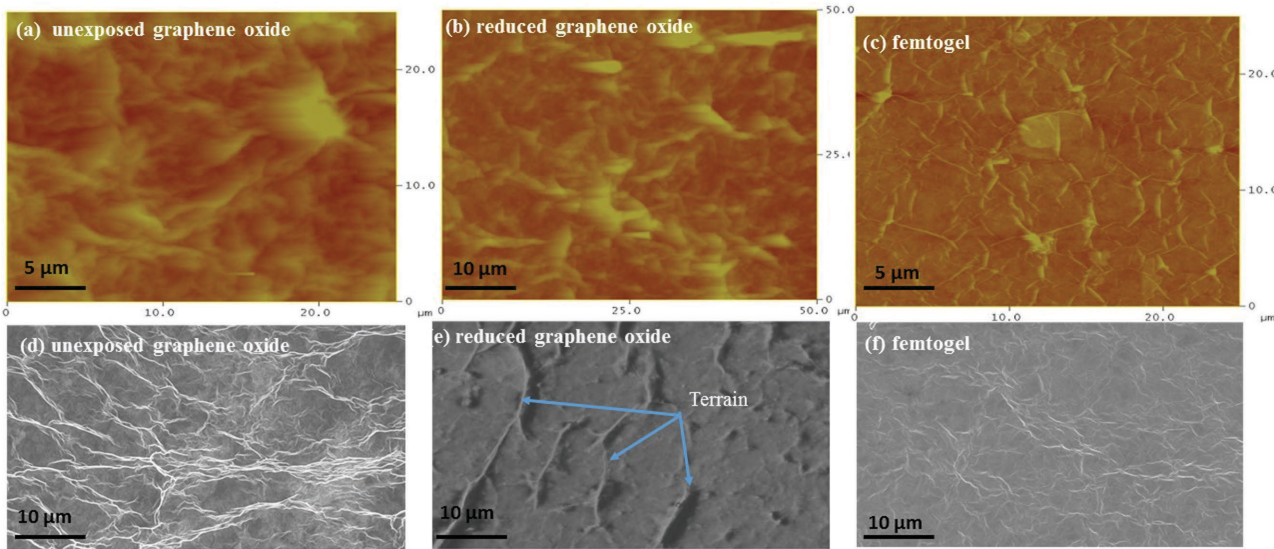


Figure 6. AFM (top row) and SEM (bottom row) images of freestanding films formed from unexposed graphene oxide, reduced graphene oxide, and the femtogel formed in 7 h. The AFM scanning range was fixed as 50 μm .

2.5. Thin Film Surface Morphologies

The surface morphologies of the thin films fabricated from unexposed graphene oxide solution, reduced graphene oxide solution and the 7 h femtogel were studied using SEM and AFM and are shown in **Figure 6**. In addition to the size of the constituent sheets/flakes, it is expected that removal of the hydroxyl and carboxyl functional groups which decorated the graphene oxide sheets will strongly affect the film morphology. Removal of these functional groups should enhance the noncovalent π - π stacking, cation- π interactions, and van der Waals forces between the sheets^[43] due to a reduction in their hydrophilic properties. Indeed, it is seen in Figure 6c and f that the surface roughness of the deposited films was minimized by converting the graphene oxide solution to a femtogel over a 7 hour period, which was shown in Figure 3a to result in a dramatically reduced OH content. The surface roughnesses of the unexposed graphene oxide and reduced graphene oxide thin films were \approx 12 and \approx 25 nm. The roughness of the deposited thin film from the 7 h femtogel was improved and recorded as 5.6 nm, which indicates that the aggregation and noncovalent binding of the small graphene oxide flakes indeed took place. Figure S6 (Supporting Information) clearly shows the stacking of the reduced graphene oxide gels sheets in the femtogel film, which is also consistent with the observed reduction in

interlayer spacing for the 7 h femtogel film. Thus by changing the beam position from inside the graphene oxide solution to the air/solution surface, femtogels were formed that can produce smoother film surfaces.

As for the other film properties measured, the surface morphology of the femtogel films was again found to depend on the gel formation parameters (e.g., laser pulse intensity and focal length). **Table 4** summarizes the measured surface roughnesses for all films, and Figures S5 and S6 in the Supporting Information display corresponding AFM and SEM images. For example, producing the femtogel in 58 min instead of 7 h (by increasing the pulse energy from 0.250 to 2 mJ) resulted in less removal of OH⁻ groups (as shown in Figure 3b) and correspondingly a much rougher film (45 nm instead of 5.6 nm). In contrast, increasing the focal length used to form a femtogel from 1.5 mL of solution from 5 to 10 cm, resulted in a faster gel formation time (8 min. vs. 20 min.), a lower OH content in the associated film (as shown in Figure 3c), and a smoother film (23 nm roughness vs. 55 nm).

3. Conclusion

We have introduced a new technique for producing reduced graphene oxide gels without any chemical agents or additives. A viscous femtogel is formed by focusing a femtosecond laser at the surface of an ultrahigh concentration single-layer flake graphene oxide aqueous solution to remove the hydroxyl and carboxyl functional groups, as well as water. Reduction of the graphene oxide and gel formation occur simultaneously, in time periods as short as a few minutes at room temperature, and dense, layered thin films can be produced using the femtogel.

Notably, varying the irradiation parameters provides control over gel formation time and gel properties. It was shown that the OH content is reduced in the femtogels, and depends on

Table 4. The surface roughness of thin films formed from unexposed graphene oxide(GO), reduced graphene oxide(rGO), and femtogels formed in the range of 8 min to 7 h, as measured by AFM.

Sample	Roughness [nm]	Sample	Roughness [nm]
GO	12.0	58 min femtogel	44.6
rGO	25.3	20 min femtogel	54.8
7 h femtogel	5.6	8 min femtogel	22.6

the laser pulse energy and focal length used. The femtogels had higher defect ratios than the unexposed graphene oxide solution, where the ratio again varied with the laser focal length, as well as the solution volume treated. Femtogels with interlayers spacing both smaller and larger than that of the graphene oxide solutions were produced, and appeared to correlate with the removal of functional groups from the graphene oxide sheets. The removal of functional groups seemed to similarly influence the morphology of films produced with the femtogels. For the longest gel formation time of 7 h, a thin film was produced with a roughness less than 6 nm and more than 95% reduction in the OH concentration (as compared to films fabricated from the unexposed graphene oxide solution).

While the ability to control the femtogel properties via the irradiation parameters has been clearly demonstrated, the complex interplay of these parameters (solution volume, focal length, pulse energy, etc.) in determining the properties merits further study. Further exploration and understanding of this parameter space will ultimately allow simultaneous optimization of relevant properties such as OH content, defect ratio, film morphology, and gel formation time for a wide variety of critical applications.

4. Experimental Section

Femtogel Fabrication: 1.5 mL and 5 mL of an ultrahigh concentration (6.2 mg mL^{-1}) single-layer graphene oxide flakes (>80%) solution with flake size of 0.5 to 5 μm (from Graphene supermarket) was exposed to femtosecond laser pulses homogeneously using a magnetic stirrer. The femtosecond laser pulses were generated by two different Ti: Sapphire regenerative amplifiers, both with a central wavelength of 800 nm and repetition rate of 1 kHz, pulse duration of 100 fs and 35 fs, and pulse energies of 250 μJ and 2 mJ, respectively. The incident laser beam was focused with either a 5 cm off axis parabolic mirror or a 10 cm focal length fused silica plano convex lens. The laser beam was focused a few millimeters inside the graphene oxide solution to produce the reduced graphene oxide and at the solution/air interface to fabricate femtogel. The laser irradiation time was varied from 8 min to 7 h as summarized in Table 1. The properties of the fabricated femtogel were compared with the unexposed and reduced graphene oxide solution. In both cases, a series of freestanding films and deposited thin films on a silicon wafer were fabricated using the filtration technique (see S1, Supporting Information) and the spin casting method, respectively.

Characterization: Raman spectroscopy was carried out for each sample using a Renishaw micro-Raman spectrometer with an excitation wavelength of 632.8 nm and power density of 4.5 mW cm^{-2} to avoid any surface modification/damages during the laser exposure and measurement. The surface morphologies and microstructure of the prepared thin films were studied using AFM, (Dimension 3100 Scanning Probe Microscope) and SEM (SEM-LEO 1530, using the Schottky-type field emission electron source). The molecular absorption of the femtogel and unexposed graphene oxide freestanding films were studied by FTIR spectroscopy (Shimadzu FTIR8400S spectrometer) in the region of 4000 to 440 cm^{-1} . The X-ray diffraction (XRD) pattern of the thin films was recorded in the range of 5° to 50° using an XPERT-PRO diffractometer system with the $K_{\alpha}1$ wavelength of 1.542 Å at 45 kV and 35 mA from an X'Pert Pro-Panalytical.

Supporting Information

Supporting Information is available from the Wiley Online Library or from the author.

Acknowledgements

K.H.I. and M.I. contributed equally to this work. M.Y. and J.S. acknowledge the support from the NSERC, Canada.

Received: December 30, 2015

Revised: February 13, 2016

Published online:

- [1] J. Wang, Z. Shi, J. Fan, Y. Ge, J. Yin, G. Hu, *J. Mater. Chem.* **2012**, *22*, 22459.
- [2] X. Yang, L. Qiu, C. Cheng, Y. Wu, Z.-F. Ma, D. Li, *Angew. Chem. Int. Ed.* **2011**, *50*, 7325.
- [3] G. Xin, T. Yao, H. Sun, S. M. Scott, D. Shao, G. Wang, J. Lian, *Science* **2015**, *349*, 1083.
- [4] H. Bai, C. Li, X. Wang, G. Shi, *Chem. Commun.* **2010**, *46*, 2376.
- [5] J. L. Vickery, A. J. Patil, S. Mann, *Adv. Mater.* **2009**, *21*, 2180.
- [6] W. Ai, Z.-Z. Du, J.-Q. Liu, F. Zhao, M.-D. Yi, L.-H. Xie, N.-E. Shi, Y.-W. Ma, Y. Qian, Q.-L. Fan, T. Yu, W. Huang, *RSC Adv.* **2012**, *2*, 12204.
- [7] D. Das, T. Kar, P. K. Das, *Soft Matter* **2012**, *8*, 2348.
- [8] C. Hou, Q. Zhang, Y. Li, H. Wang, *Carbon* **2012**, *50*, 1959.
- [9] S.-Y. Qin, X.-J. Liu, R.-X. Zhuo, X.-Z. Zhang, *Macromol. Chem. Phys.* **2012**, *213*, 2044.
- [10] Y. Xu, K. Sheng, C. Li, G. Shi, *ACS Nano* **2010**, *4*, 4324.
- [11] W. Chen, S. Li, C. Chen, L. Yan, *Adv. Mater.* **2011**, *23*, 5679.
- [12] S. Wang, Y. Zhang, N. Abidi, L. Cabrales, *Langmuir* **2009**, *25*, 11078.
- [13] Y. Xu, Q. Wu, Y. Sun, H. Bai, G. Shi, *ACS Nano* **2010**, *4*, 7358.
- [14] C. N. R. Rao, A. K. Sood, *Graphene: Synthesis, Properties, and Phenomena*, Wiley-VCH, Germany **2013**.
- [15] S.-Z. Zu, B.-H. Han, *J. Phys. Chem. C* **2009**, *113*, 13651.
- [16] Y. Xu, H. Bai, G. Lu, C. Li, G. Shi, *J. Am. Chem. Soc.* **2008**, *130*, 585.
- [17] H. Bai, C. Li, X. Wang, G. Shi, *J. Phys. Chem. C* **2011**, *115*, 5545.
- [18] J. Chen, K. Sheng, P. Luo, C. Li, G. Shi, *Adv. Mater.* **2012**, *24*, 4569.
- [19] O. C. Compton, Z. An, K. W. Putz, B. J. Hong, B. G. Hauser, L. C. Brinson, S. T. Nguyen, *Carbon* **2012**, *50*, 3399.
- [20] V. P. Kandidov, O. G. Kosareva, I. S. Golubtsov, W. Liu, A. Becker, N. Akozbek, C. M. Bowden, S. L. Chin, *Appl. Phys. B* **2003**, *77*, 149.
- [21] R. Saito, A. Jorio, A. G. Souza Filho, G. Dresselhaus, M. S. Dresselhaus, M. A. Pimenta, *Phys. Rev. Lett.* **2001**, *88*, 027401.
- [22] Y. Sato, T. Kodama, H. Shiromaru, J. H. Sanderson, T. Fujino, Y. Wada, T. Wakabayashi, Y. Achiba, *Carbon* **2010**, *48*, 1673.
- [23] H.-W. Chang, Y.-C. Tsai, C.-W. Cheng, C.-Y. Lin, P.-H. Wu, *Electrochim. Commun.* **2012**, *23*, 37.
- [24] L. Huang, Y. Liu, L.-C. Ji, Y.-Q. Xie, T. Wang, W.-Z. Shi, *Carbon* **2011**, *49*, 2431.
- [25] D. Tan, X. Liu, Y. Dai, G. Ma, M. Meunier, J. Qiu, *Adv. Opt. Mater.* **2015**, *3*, 836.
- [26] D. Tan, S. Zhou, J. Qiu, N. Khusro, *J. Photochem. Photobiol. C* **2013**, *17*, 50.
- [27] D. Tan, Y. Yamada, S. Zhou, Y. Shimotsuma, K. Miura, J. Qiu, *Nanoscale* **2013**, *5*, 12092.
- [28] R. C. Banks, *Bonding and Hybridization*, https://chemistry.boisestate.edu/richardbanks/inorganic/bonding%20and%20hybridization/bonding_hybridization.htm, May 2002.
- [29] K. M. Ibrahim, *Femtosecond Laser Interaction with Graphene Oxide Aqueous Solution*, University of Waterloo, Waterloo, Ontario **2015**.
- [30] J. Oh, J.-H. Lee, J. C. Koo, H. R. Choi, Y. Lee, T. Kim, N. D. Luong, J.-D. Nam, *J. Mater. Chem.* **2010**, *20*, 9200.

- [31] B. Faust, in *Modern Chemical Techniques: An Essential Reference for Students and Teachers*, Royal Society Chemistry, London, **1997**, Ch. 3.
- [32] I. Jung, D. A. Dikin, R. D. Piner, R. S. Ruoff, *Nano Lett.* **2008**, *8*, 4283.
- [33] R. Trusovas, K. Ratautas, G. Račiukaitis, J. Barkauskas, I. Stankevičienė, G. Niaura, R. Mažeikienė, *Carbon* **2013**, *52*, 574.
- [34] A. C. Ferrari, J. C. Meyer, V. Scardaci, C. Casiraghi, M. Lazzeri, F. Mauri, S. Pisacane, D. Jiang, K. S. Novoselov, S. Roth, A. K. Geim, *Phys. Rev. Lett.* **2006**, *97*, 187401.
- [35] A. C. Ferrari, J. Robertson, *Phys. Rev. B* **2000**, *61*, 14095.
- [36] B. Butz, C. Dolle, F. Nielke, K. Weber, D. Waldmann, H. B. Weber, B. Meyer, E. Spiecker, *Nature* **2014**, *505*, 533.
- [37] S. Eigler, C. Dotzer, A. Hirsch, *Carbon* **2012**, *50*, 3666.
- [38] L. G. Cançado, A. Jorio, E. H. M. Ferreira, F. Stavale, C. A. Achete, R. B. Capaz, M. V. O. Moutinho, A. Lombardo, T. S. Kulmala, A. C. Ferrari, *Nano Lett.* **2011**, *11*, 3190.
- [39] T. Szabó, O. Berkési, P. Forgó, K. Josepovits, Y. Sanakis, D. Petridis, I. Dékány, *Chem. Mater.* **2006**, *18*, 2740.
- [40] M. Herrera-Alonso, A. A. Abdala, M. J. McAllister, I. A. Aksay, R. K. Prud'homme, *Langmuir* **2007**, *23*, 10644.
- [41] C. Xu, X. Wu, J. Zhu, X. Wang, *Carbon* **2008**, *46*, 386.
- [42] M. M. Cooper, M. W. Klymkowsky, in *CLUE: Chemistry: Life, the Universe and Everything*, Colorado University, Boulder **2012**, <http://virtual-laboratory.colorado.edu/clue-chemistry>, Ch. 3.
- [43] D. R. Dreyer, S. Park, C. W. Bielawski, R. S. Ruoff, *Chem. Soc. Rev.* **2010**, *39*, 228.

Copyright WILEY-VCH Verlag GmbH & Co. KGaA, 69469 Weinheim, Germany, 2016.



Supporting Information

for *Adv. Mater. Interfaces.*, DOI: 10.1002/admi.201500864

A Novel Femtosecond Laser-Assisted Method for the Synthesis of Reduced Graphene Oxide Gels and Thin Films with Tunable Properties

*Khaled H. Ibrahim, Mehrdad Irannejad, * Mojtaba Hajialamdar, Ali Ramadhan, Kevin P. Musselman, Joseph Sanderson, and Mustafa Yavuz*

Copyright WILEY-VCH Verlag GmbH & Co. KGaA, 69469 Weinheim, Germany, 2013.

Supporting Information

A novel femtosecond laser assisted method for the synthesis of reduced graphene oxide gels and thin films with tunable properties

Khaled H. Ibrahim, Mehrdad Irannejad*, Mojtaba Hajialamdar, Ali Ramadhan, Kevin P. Musselman, Joseph Sanderson, Mustafa Yavuz

S1. Thin film fabrication techniques

The unexposed graphene oxide, reduced graphene oxide and femtogel freestanding films were fabricated using the vacuum filtration technique.^[1] A Whatman Anodisc filter membrane of 0.02 µm pore size was mounted on a vacuum system using a Buchner funnel and flask (**Figure S1a**). 0.5 mL of the graphene oxide solution, reduced graphene oxide solution and femtogel were placed gently on the filter membrane to ensure the water content is vacuumed through the openings of the filter pores. The membrane was then baked for 6 hours at 50 °C inside an oven to evaporate any excess water within the filtered film (Figure S1b). Separation of fabricated films from the membrane filter was carried out by means of etching using 37% diluted hydro-chloric acid (Figure S1c). The freestanding film was then lifted off from the etching solution and kept inside the vacuum oven to dry as shown in Figure S1d and was kept in a vacuum desiccator.

A series of thin films were also fabricated on Si substrates using the spin casting technique with a speed of 3000 rpm for 30 seconds, followed by a 20 min post-baked at 90 °C in order to remove thermal stress and increase the adhesion between the film and substrate. The fabricated thin films, were then slowly cooled down to room temperature to minimize the thermal stress.

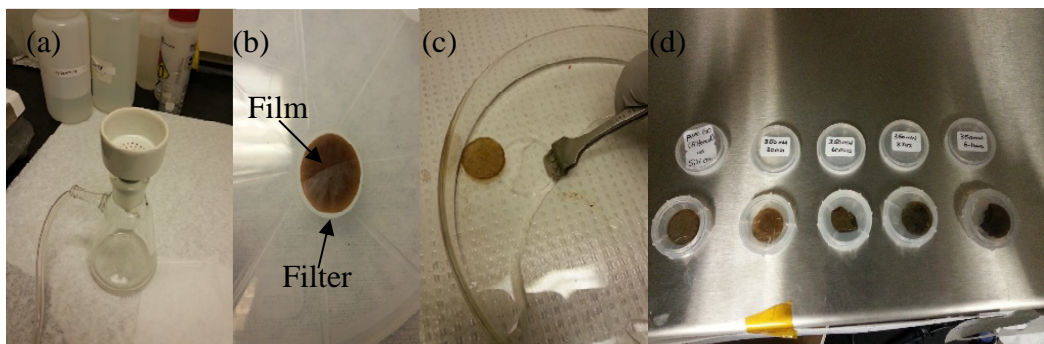


Figure S1. (a) Buchner funnel and flask connected to vacuum system, (b) filtered film on the membrane after post baking (c) etched freestanding film from membrane in 37 % diluted HCl, (d) dried freestanding film in the vacuum oven.

S2. FTIR spectroscopy of femtogel

Figure S2 shows the recorded FTIR transmission spectra of freestanding films fabricated with unexposed graphene oxide and femtogel formed in the range of 8 minutes to 7 hours. The dominant features were recorded at 3381 cm^{-1} , 1740 cm^{-1} , 1623 cm^{-1} , 1402cm^{-1} - 1423 cm^{-1} , 1260 cm^{-1} , 1075 cm^{-1} , 860 cm^{-1} and 1570 cm^{-1} which are assigned to the stretching OH, stretching C=O, C=C, C-OH, C-O-C, stretching C-O and the bending C-H vibration bonds respectively.^[2-5]

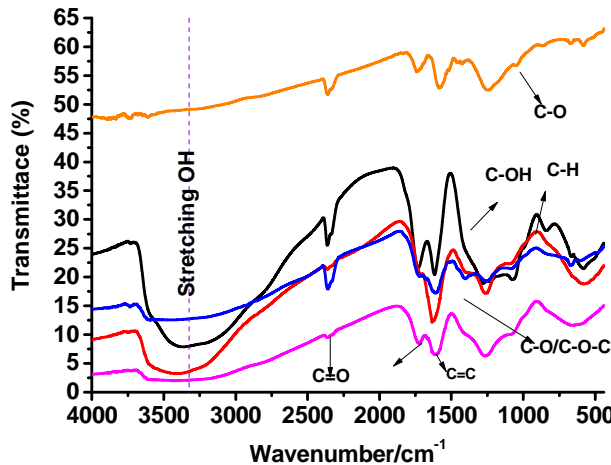


Figure S2. The recorded transmittance FTIR spectra of freestanding films fabricated from (—) unexposed graphene oxide solution, (—) femtogel formed in 8 minutes, (—) femtogel formed in 20 minutes, (—) femtogel formed in 58 minutes and (—) femtogel formed in 7 hours.

From this figure, it is clear that the sp^2 bonded $\text{C}=\text{C}$ (1623 cm^{-1})^[6] is still the most prominent peak in all the spectra and offers the strongest absorbance peaks amongst all carbonic features in the recorded unexposed graphene oxide and femtogel spectra. It was found that the freestanding film fabricated from the femtogel formed in 8 minutes has a larger amount of the $\text{C}=\text{C}$ molecular bonds, as was also confirmed by XPS analysis (**Figure S3**). This observation could be attributed to the shorter irradiation time compared to the other femtogels formed in the range of 20 minutes to 7 hours, which resulted in a smaller amount of graphene oxide flakes/sheets fractures into small graphene oxide flakes, such that a larger amount of $\text{C}=\text{C}$ molecular bonds are preserved. The absorbance intensity of the $\text{C}-\text{OH}$ molecular bond ($1402\text{-}1423 \text{ cm}^{-1}$)^[6] was completely reduced in the femtogel freestanding films by increasing the irradiation time as shown in Figure S2. The bridging oxygen ($\text{C}-\text{O}-\text{C}$ bond, 1260 cm^{-1})^[7] becomes more prominent by increasing the irradiation time, which can be attributed to the reaction of an oxygen atom (with two lone pair electrons) with two carbon atoms (with single lone pair electrons from $\text{C}=\text{C}$ bonds broken during the laser irradiation).

The bending C-H bond (860 cm^{-1} and 1570 cm^{-1})^[7] was disappeared in all femtogel freestanding films, as is evident from Figure S2. This could be due to the dissociation of the weak C-H bond and hence the formation of water vapor as a result of reactions between the hydrogen ions and free OH⁻ ions.

It can be concluded that extending the irradiation time to 7 hours after femtogel formation results in more OH⁻ groups removal from the basal plane, as observed by the absence of the OH⁻, C-H and C-OH bonds from the recorded FTIR spectrum (orange curve) in Figure S2.

S3. X-ray photoluminescence analysis of femtogel thin films deposited on Si substrates

The XPS spectra of the C1s transition of the unexposed graphene oxide thin film and thin films fabricated from femtogels formed in the range of 8 minutes to 7 hours are compared in Figure S3. As can be seen from Figure S3, the unexposed graphene oxide spectra includes a peak corresponding to the COOH (290.5 eV)^[8] molecular bond, whereas this peak was not present for the femtogels formed in the range of 8 minutes to 7 hours, consistent with the removal of OH⁻ groups from the femtogels, as observed by FTIR spectroscopy. Figure S3 shows that with laser irradiation the intensity of the C-C peak was decreased relative to the intensity of the C-O peak, which is attributed to more production of sp³ hybridization features by dissociation of the sp² bonds as a result laser irradiation and the fracture of graphene oxide sheets to smaller sheets/flakes. The increases in the recorded intensity of C-O bond is in agreement with the Raman results discussed in section 2.3. The presence of the oxygen atoms on the periphery of the graphene sheets helps in the aggregation of the femtogel networks by means of oxygen bridging and C-O-C bond formation which was confirmed by recording the C-O bond with larger intensity.

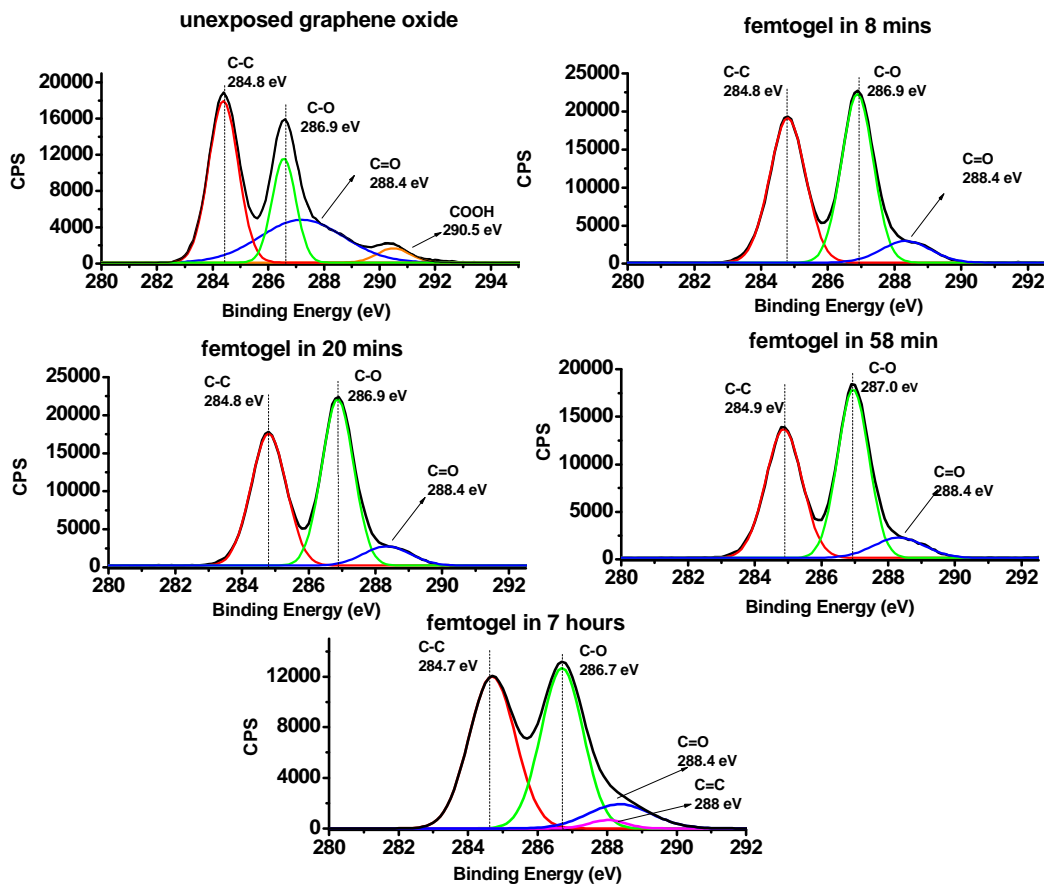


Figure S3. Recorded XPS spectra of C1s transition in the fabricated thin films from unexposed graphene oxide solution and femtogel formed in the range of 8 minutes to 7 hours.

S4. Surface morphology of femtogel films deposited on the Si substrate.

Figure S4 shows the AFM images of an unexposed graphene oxide thin film, reduced graphene oxide thin film, and thin films formed from femtogels. It was found that the thin films deposited from femtogels formed in 8 minutes, 20 minutes and 58 minutes possessed larger surface roughness, indicating an irregularity in the stacking of the graphene oxide sheets relative to the unexposed graphene oxide and femtogel formed in 7 hours.

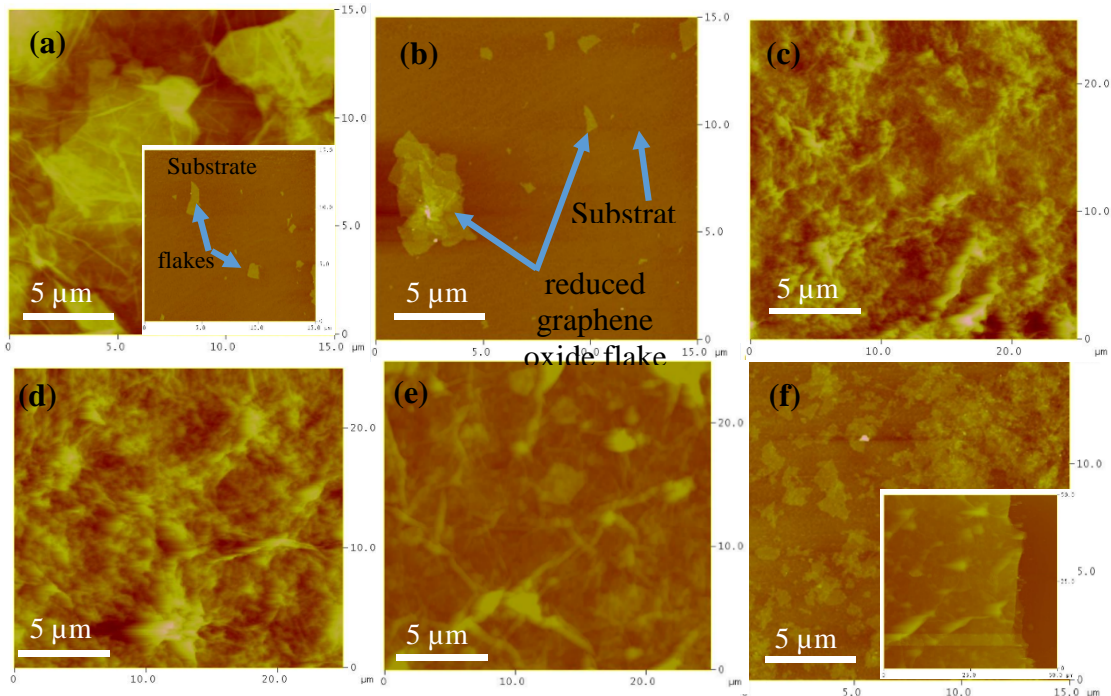


Figure S4. AFM images from fabricated thin films of (a) unexposed graphene oxide, (b) reduced graphene oxide, and femtogels formed in (c) 8 minutes, (d) 20 minutes, (e) 58 minutes, and (f) 7 hours. Insets show scans from different positions on the same sample.

The SEM images of films fabricated from femtogels are compared in **Figure S5**. The SEM images confirm a smoother surface for the femtigel formed in 7 hours. The wrinkled layers are common features in the thin films fabricated from femtogels formed in the range of 8 minutes to 7 hours as also evident from Figure S5. The extent of the wrinkles/folding features was greater for gel formation conditions that removed fewer oxygen functional groups, which decorate the graphene oxide flakes in the graphene oxide solution and femtogels. These remaining functional groups caused the stacked graphene oxide flakes to become thicker than that of the femtigel formed in 7 hours where the oxygen content was minimized (as shown in the FTIR spectra) and the film surface was much smoother.

Figure S6 shows the SEM image of an induced crack in the thin films formed from 7 hour femtogel. It is clear that these films consist of stacked graphene oxide sheets.

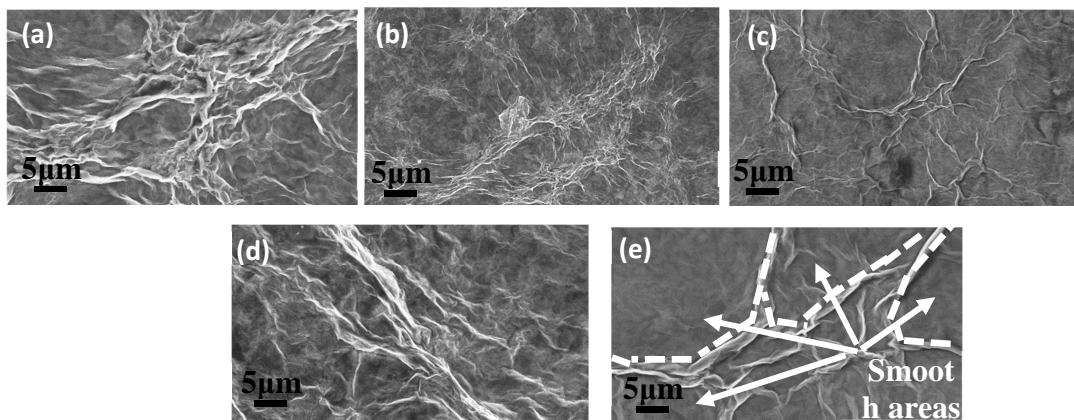


Figure S5. The SEM images of thin films fabricated from (a) unexposed graphene oxide solution, and femtogels formed in (b) 8 minutes (c) 20 minutes, (d) 58 minutes and (e) 7 hours on a Si substrate.

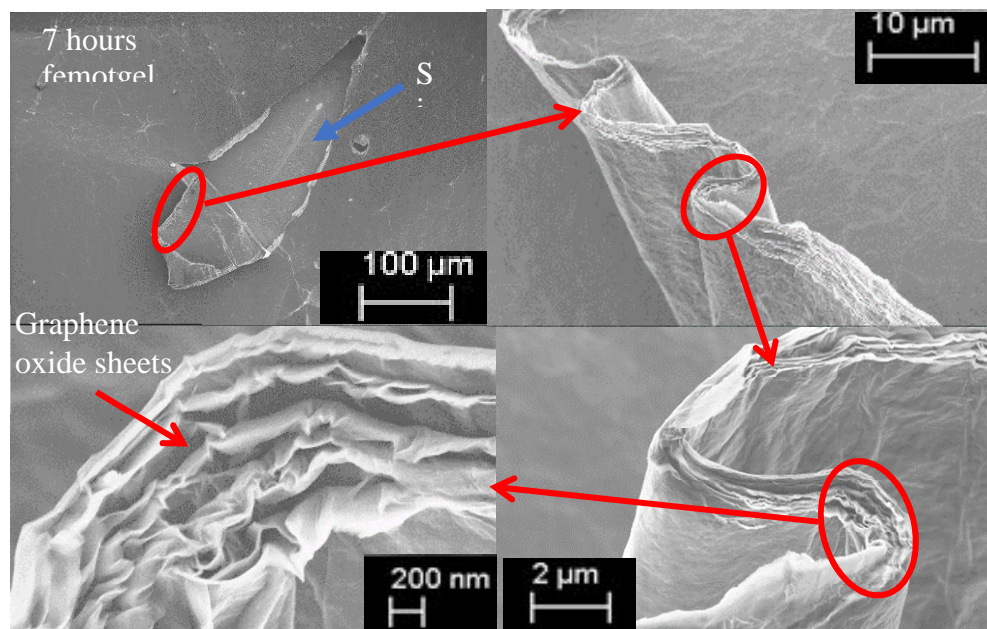


Figure S6. SEM image of an induced crack in the thin film fabricated from femtogel formed in 7 hours, which clearly shows the layered stacking of graphene oxide sheets.

- [1] J. Chen, Y. Guo, L. Huang, Y. Xue, D. Geng, H. Liu, B. Wu, G. Yu, W. Hu, Y. Liu, D. Zhu, *Phil. Trans. R. Soc. A* **2013**, 372.
- [2] J. Oh, J.-H. Lee, J.C. Koo, H.R. Choi, Y. Lee, T. Kim, N.D. Luong, J.-D. Nam, *J. Mater. Chem.* **2010**, 20, 9200.
- [3] X.-k. Kong, Q.-w. Chen, Z.-y. Lun, *J. Mater. Chem. A* **2014**, 2, 610.
- [4] W. Ai, Z.-Z. Du, J.-Q. Liu, F. Zhao, M.-D. Yi, L.-H. Xie, N.-E. Shi, Y.-W. Ma, Y. Qian, Q.-L. Fan, T. Yu, W. Huang, *RSC Adv.* **2012**, 2, 12204-12209.
- [5] H. Zhang, D. Hines, D.L. Akins, *Dalton Transactions* **2014**, 43, 2670.
- [6] K. Krishnamoorthy, M. Veerapandian, K. Yun, S.J. Kim, *Carbon* **2013**, 53, 38.
- [7] H.N. Lim, N.M. Huang, S.S. Lim, I. Harrison, C.H. Chia, *Int.J. Nanomed.* **2011**, 6, 1817.
- [8] Y. Sato, T. Kodama, H. Shiromaru, J.H. Sanderson, T. Fujino, Y. Wada, T. Wakabayashi, Y. Achiba, *Carbon* **2010**, 48, 1673.